Biogeosciences Discuss., https://doi.org/10.5194/bg-2017-222
Manuscript under review for journal Biogeosciences
Discussion started: 7 June 2017

Biogeosciences Discussions Open Access EGU

Continuous fluorescence-based monitoring of seawater pH in a temperate estuary

John W. Runcie[1,2,3], Christian Krause[4], Sergio A. Torres Gabarda[1,3]. Maria Byrne[1,3]

[1]School of Life and Environmental Sciences, University of Sydney, Sydney, Australia
[2]Aquation Pty Ltd, Umina Beach, Australia,
[3]Sydney Institute of Marine Sciences, Mosman, Australia
[4]Presens Precision Sensing GmbH, Regensburg, Germany

Correspondence to: John W. Runcie (john.runcie@sydney.edu.au)

Abstract. Electrical conductivity (salinity), temperature and fluorescence-based measurements of pH were employed to examine diel fluctuations in seawater carbonate chemistry of surface waters in Sydney Harbour over two multiple-day periods. The fluorescence-based technique provided a useful time-series for pH. Alkalinity with pH and temperature were used to calculate the degree of aragonite and calcite saturation (Ω_{Ca} and Ω_{Ar} respectively). Alkalinity was determined from an alkalinity-salinity relationship. Variation in pH over minute- to hour-long periods was distinguishable from background variability. Diel variability in pH, Ω_{ara} and Ω_{cal} showed a clear pattern that appeared to correlate with both salinity and temperature. Drift due to photodegradation of the fluorophore was minimised by reducing exposure to ambient light. Ω_{Ca} and Ω_{Ar} fluctuated approximately on a daily cycle. The net result of changes in pH, salinity and temperature combined to influence seawater carbonate chemistry. The fluorescence-based pH monitoring technique is simple, provides good resolution and is unaffected by moving parts or leaching of solutions over time. The use of optics is pressure insensitive, making this approach to ocean acidification monitoring well suited to deepwater applications.

1 Introduction

Ocean carbon chemistry is predicted to vary in response to elevated atmospheric [CO_2], with a decline in pH and an increase in dissolved CO_2 (pCO_2) over the coming decades. However, short-term diel changes in seawater pH and pCO_2 at the scale of an embayment are unlikely to represent predicted globally increasing trends. Seawater carbonate chemistry in shallow nearshore environments is more likely driven by a combination of biological (photosynthesis, respiration) and local hydrodynamic (tidal, low salinity surface- and/or ground-water input) processes (Santos et al. 2012) with typical variation at time scales ranging from minutes to days. Capturing these short-term fluctuations requires virtually-continuous monitoring of water chemistry.

Seawater pH has until recently been largely measured using glass electrodes. While accurate and precise, this technology suffers from a gradual loss of electrolyte and consequent drift, requiring recalibration. In addition, ion selective electrodes are susceptible to poisoning, in particular by sulphide released when conditions become anoxic. However, recent advances in electrode design including the incorporation of more internal salt bridges have enabled the continuous use of glass pH electrodes in shallow marine waters for over 12 months (Ionode Pty Ltd, Australia, pers. comm).

Ion selective field effect transistor (ISFET) technology is becoming more widely used to measure pH in seawater. pH sensors using ISFET technology comprise the ISFET sensor itself - a solid-state device with a H+ ion sensitive material, a counter electrode and a reference electrode. In pH monitoring systems such as the SeaFET (Martz et al. 2010, Takeshita et al. 2015, Johnson et al, 2016) a chloride electrode is used as reference as chloride ion activity is relatively constant in deep water. However this introduces problems in locations where chloride concentrations fluctuate, such as euryhaline estuarine environments.

Optical fluorescence-based approaches to pH sensing offer an alternative to glass electrodes and ISFET sensors. Optical methods do not require electrolyte solutions or gels which gradually lose ions, nor do they require reference electrodes and their accompanying susceptibility to varying environmental conditions. Optical methods are also impervious to high pressure, only the housing for the device and the window through which the optical signal is passed must be pressure resistant. The use of fluorescence lifetimes measurements provides the additional advantage of being insensitive to changes in fluorescence intensity.

In this study we explore a new approach to logging pH in seawater and in the setting of an estuarine environment. We incorporated a commercially available fluorescence-based pH sensing system (Presens GmbH) in a submersible continuous monitoring device (Aquation Pty Ltd) to measure short term changes in seawater pH in surface waters in Sydney Harbour over two multi-day intervals in Autumn and Summer. Electrical conductivity and temperature were also measured, and alkalinity was derived from a salinity-alkalinity relationship reported for the Australasian region (Lenton et al. 2016). With these data we estimated changes in seawater carbonate chemistry during the deployments. The objectives of the study were to a) characterise the fluorescence-based pH monitoring system in seawater in terms of stability and resolution, and b) to characterise diel fluctuations of pH and aragonite/calcite saturation state in surface waters.

2 Methods

2.1 Study site and sampling arrangements

Real-time seawater measurements were made of seawater in the Sydney Harbour estuary at the Sydney Institute of Marine Sciences (SIMS), Chowder Bay (-33.839357 °S, 151.254587 °E) (Fig. 1). Chowder Bay is a shallow (5 to 10 m) embayment

located on the northern shore of Sydney Harbour some 3 km from the ocean. Tides in Sydney Harbour (depths typically ~20 m) are semi-diurnal, with a maximum difference of 1.95 m at the estuary entrance. Tidal fluctuation during the deployment intervals is referenced to measurements made at nearby Fort Denison (Caldwell et al. 2015). Seawater chemistry was measured from approximately 1 m below sea level at low tide below the SIMS pier at Chowder Bay.

Two field deployments were conducted. Firstly, water was collected some 1-2 m below sea level at low tide and pumped 3-5 m up into a 2 L reservoir in an enclosed structure at the end of the wharf. Water exited the reservoir through a narrow tube located below an overflow pipe at the upper part of the reservoir, passing through a clear polycarbonate tube for optical measurement (*ex situ* measurements, Autumn, 8th-19th April 2016). Fluorescence spots were attached to the inside of this tube and a plastic optical fibre was positioned perpendicular to the outside of the tube and directed to the spot. To avoid photobleaching the system was covered in black plastic eliminating most light. Waste water was directed back into the harbour at least 5 m away from the intake location. This series of tests enabled us to make frequent measurements as the system could use a constant supply of mains power.

In situ measurements were made ~1 m below low tide during 14th-22nd December 2016, with the self-contained instrument attached vertically to a pier under the wharf and the fluorescence spot facing downwards to minimise sunlight-induced photobleaching (Fig. 2). In this arrangement the plastic optical fibre within the clear polycarbonate cylindrical housing of the instrument was oriented perpendicular to the faceplate. To ensure that the spot could not peel off, a non-fluorescent mesh was held in place over the spot with a plastic ring. This arrangement ensured that the spot was fixed in position and water could easily reach the fluorophore and respond to ambient pH. A small hole was drilled partway into the inside of the faceplate to bring the fibre tip closer to the spot, which was affixed to the external surface of the faceplate. This was necessary to increase signal strength to an acceptable level. During the *in situ* measurements, water samples were collected adjacent to the instrument and removed to the laboratory for measurement of pH_T (see below) within 30 minutes of sampling. The instrument contained three NiMH battery packs in series comprising 14 cells each with a total of 13.5 Ah at 16.8 volts.

2.2 pH measurements

The fluorescence-based pH measurement uses a dual-luminophore frequency-domain fluorescence decay technique (Huber et al. 2001). A pH sensitive dye with short fluorescence decay time which changes its fluorescence intensity dramatically with pH is mixed together with an inert reference dye with long decay time. Both dyes are immobilized in particles which are dispersed in a hydrophilic membrane. This sensing membrane is in contact with the ambient water and a light guide is brought to the opposite site of the membrane to read the pH (Fig. 3). The read out unit (EOM-pH-mini) sends sine-wave modulated blue light to excite both dyes simultaneously (the "spot") and measures the average decay time of the sum of returned fluorescence light from both dyes.

Calibration was performed prior to deployment of the instrument. All glassware, buffers, seawater and the instrument were left overnight in an air-conditioned room to reach a stable temperature of 22 °C. An Ag/AgCl pH electrode (Ionode Pty Ltd) was calibrated against standard buffers (pH 7.02 and 10.06 at 20° C). A pair of phosphate buffer solutions were also prepared, isotonic to ~34.5 ppt NaCl (I = 0.7 M) with C1=8.33 pH and C2=4.00 pH (where C1 and C2 are the measured pH of each of the buffers). A small volume (e.g. 0.25 mL) of C1 was added to 10 mL of C2 until the combined buffer reach a pH of 4.45 as measured by the Ag/AgCl electrode. An aliquot (approx. 1 mL) of this combined buffer solution of known pH was pipetted onto the fluorescence spot (fixed to the inside of the clear polycarbonate tube, or fixed to the faceplate of the instrument) and the fluorescence phase measured. Settling time of the phase value for each aliquot could take at least 10 minutes. Then, more C1 was added to the combined buffer and the process repeated at pH 5.66, 6.81, 7.23, 7.72, 8.02 and 8.30. The relationship between measured phase and (total) pH was determined with a non-linear Boltzman sigmoid model using the software provided by the manufacturer. We did not use Tris as a buffer as it is known to poison single junction Ag/AgCl electrodes.

During the *in situ* deployment, water samples were collected by swimmer adjacent to the pH monitor when underwater and transported to the nearby lab at SIMS in 200 mL glass jars. Within 30 minutes of collection, pH was measured spectrophotometrically with *m*-cresol purple indicator dye (Acros Organics, Lot # A0321770) using a custom-built automated system with a USB4000 fibre optic spectrophotometer (Ocean Optics) following SOP 6b from (Dickson et al., 2007) and calculations from Liu et al. (2011). Spectrophotometric measurements of pH_T were validated using seawater certified reference material (CRM, Dickson Standard Batch 145). The measured pH_T was compared to the calculated pH_T of the CRM using published values for total alkalinity (A_T), dissolved inorganic carbon (DIC) and salinity at the same temperature.

The gradual drift experienced with the fluorescence-based pH sensor was then corrected assuming a linear decline in measured pH corresponding with photodegradation of the fluorophore spot, which was shaded but not in the dark. Corrections were made against the reference samples measured spectrophotometrically, as described previously.

Ex situ and *in situ* measurements were taken once per minute or 10 times in one minute every 10 minutes, respectively, and a running average of 10 minutes of the *ex situ* measurements is presented. *In situ* measurements taken over one minute were averaged before analysis.

2.3 Temperature

PT100 sensors were either suspended in the 2L reservoir that received seawater immediately prior to measurement, or were simply positioned up against the inside of the housing wall when deployed *in situ*. Initial temperature data during the *in situ* deployment were ignored until the sensors reached equilibrium with ambient water. *Ex situ* and *in situ* measurements were

taken twice every minute, or 10 times in one minute every 10 minutes, respectively. Sets of two or 10 measurements were averaged before analysis and a running average of 10 minutes of the *ex situ* measurements is presented.

2.4 Salinity

Electrical conductivity was measured using a Hanna HI3001 four ring potentiometric conductivity probe designed for flow-through sensing wired to a custom circuit board. Millivolt values were converted to salinity assuming a linear relationship between sensor readings and salt content. The sensor was calibrated against a pure NaCl solution of known concentration at temperatures similar to that expected of seawater at the sampling location. *Ex situ* and *in situ* measurements were taken three times per minute every minute, or 10 times in one minute every 10 minutes, respectively, and these sets of three or 10 measurements were averaged before analysis. A running average of 10 minutes of the *ex situ* measurements is presented

2.5 Datalogging and calculations

Both flow-through and *in situ* deployments were conducted using a custom datalogger/controller system based on a Submersible Datalogger (Aquation Pty Ltd, Australia). All data were saved on board and downloaded to PC after retrieval of the instrument. Alkalinity was calculated from salinity data according to a linear salinity-alkalinity relationship for Australasian waters described by Lenton et al. (2016). Corrections were made to the raw data if required, and final pH, pCO2, temperature and alkalinity values were used to calculate Ω_{Ca} and Ω_{Ar} in CO2Sys (V2.1) (Dickson and Millero 1987).

3.0 Results

3.1 pH

Seawater collected and pumped to the sensor varied by 0.08 pH units from 7.97 to 8.05 over the three-day interval in Autumn (Fig. 4). The precision of calculated pH was 0.022 pH units. This is constrained by the resolution (0.01°) and precision (0.05°) of the lifetimes-decay fluorometer. The best precision can be achieved by averaging multiple measurements. Gradual photodegradation is known to influence fluorophores, contributing to a steady drift. In this case, the decline in pH was 0.0136 pH units per day. pH measured over summer ranged from 7.95 to almost 8.15 units, some 0.1 units more basic than Autumn values (Fig. 5).

3.2 Temperature

Temperature fluctuated between 21.6°C and 22.6°C in April (*ex situ* measurements, Fig. 4), and 21.0 to 23.6 in December (*in situ* measurements, Fig. 5). The stated resolution of the PT100 temperature sensors was 0.01°C and concurrent readings were within 0.05 °C of each other. Over the three day period, temperature showed a consistent pattern of declining at night and then rapidly increasing again around the middle of the day, reaching a maximum value around mid-afternoon. During the *in situ* deployment, diel fluctuations in ambient seawater temperature varied between 1 and 2 degrees, and increased to 23.6°C in the last two days of the measuring interval (Fig. 5).

3.3 Salinity

Salinity was calculated from electrical conductivity, and ranged from 33.0 to 34.3 psu during the *ex situ* measurements, and 34.6 to 37.7 during the *in situ* measurements with a mean value of approximately 36.5 psu during the *in situ* measurements (Figs 4 and 5 respectively). Diel variation roughly tracked the tidal cycle with higher salinity driven by the incoming tide. However, the amplitude of the salinity signal was not driven by the tidal amplitude (Fig. 4).

3.4 Saturation states

Both Ω_{ara} and Ω_{cal} calculated from water in the *ex situ* trial fluctuated over the course of three days, appearing to provide a smoothed approximation of diel variation in these three parameters (Fig. 6). Most striking is the noise associated with the calculated values, reaching as high as 1 Ω units. Ω_{ara} appeared to have slightly less variability than Ω_{cal}. Ω_{ara} varied between approximately 2.5 and 3.1 units, while Ω_{cal} varied from approximately 3.8 to 5.4 units (Fig. 6). Saturation state values also shifted approximately on a 24 hour cycle, with higher values roughly synchronising with 1800 hours (Figs 6 and 7).

4.0 Discussion

4.1 Instrumentation

The fluorescence-based pH measurements provide sufficient resolution to observe and predict diel changes in nearshore system pH, and indicated significant changes in seawater /carbonate chemistry at timescales of hours to days. Values of pH, salinity and temperature were all within what one would expect for the harbour at that time of year. Further, the average magnitude of both Ω_{cal} and Ω_{ara} were within the bounds of expected values for current-day marine surface waters.

The mains-powered instrument designed to measure water pumped up from the harbour had the advantage of unlimited power and the capacity to make multiple measurements several times per minute. However, the dissolved gas content of

pumped water can vary relative to the source water, making measurements less representative of the water to be sampled. We kept this to a minimum by pumping water over a short distance. Further, the need to use a suitable secure location with a constant power source is a limitation with respect to field deployments. On the other hand, the self-powered instrument tested during December 2016 had sufficient power to operate unattended for several weeks, and with a decrease in sampling frequency the lifetime of the unit could be extended to several months. For even longer periods the device could be constructed using a longer cylinder, a separate battery pack, with lithium ion batteries, or combinations of these. With this approach, the unit could be powered to operate unattended for over 12 months.

The housing used in this study was constructed from 5 mm thick acrylic. However, calculations indicate failure of the housing at depths exceeding 100 m. A metal housing with regular bulkheads along its length would increase pressure resistance and provide an instrument capable of withstanding deep ocean pressures.

4.2 Data and significance

While there was a clear diel fluctuation in temperature of about 1 °C both in December and April, the gradual increase in temperature during the 20th and 21st of December (austral Summer) was coincident with a decline in salinity and tidal amplitude (Fig. 5). This suggests an influx of warmer freshwater into the estuary coupled with weaker tidal pumping, where pumping corresponds with flushing of the harbour with higher-salinity seawater from the ocean. pH, Ω_{cal} and Ω_{ara} also declined during these last two days of the deployment. These data show that temperature and salinity play an important role in seawater carbonate chemistry, as is well known (Millero 1995). As a consequence of these physical factors (and presumably photosynthesis and respiration; Schulz and Riebesell, 2013), nearshore coastal waters and estuaries experience changes in Ω_{cal} and Ω_{ara} not only over the course of several days, but also over a 24 hour period. This contrasts with oceanic marine waters that maintain relatively constant values of saturation state. Models used to forecast seawater carbonate chemistry, such as those employed in the IPCC reports are typically based on the open ocean. The projections for the open ocean do not incorporate the short-term fluctuations typical of coastal waters (Hendriks et al. 2015).

However, when assessing nearshore shallow-water marine coastal and estuarine environments, these short-term fluctuations in seawater carbonate chemistry can be significant, as found in this study, and are best accounted for and included in predictive models. Perhaps most important is to determine the capacity for organisms that live in these highly fluctuating environments to withstand or thrive in spite of such a regular chemistry change. Here we generated a targeted data set to assess the application of the fluorescence based method. Our results show the influence of fluctuating temperature and salinity on saturation state in an estuarine environment. More research is needed to determine in detail these and other drivers of fluctuating saturation states (e.g. photosynthesis and respiration), and the actual consequences of these changes to key resident marine species.

4.3 Conclusion

We observed pH of surface water at Chowder Bay in Sydney Harbour to vary significantly across a diel cycle, influenced by temperature, salinity and tidal height /alternating freshwater or saline dominance. The fluorescence-based pH monitoring technique used here could resolve changes in pH to 0.022 pH units. Corresponding saturations states of calcite and aragonite (Ω_{cal} and Ω_{ara}), calculated from pH, temperature and salinity-derived alkalinity values showed diel fluctuations in seawater carbonate chemistry that can be interpreted as the combined effect of pH, temperature and salinity. Variability in saturation state over such short time scales in this shallow ecosystem indicates the importance of high temporal and spatial resolution measurements of seawater carbonate chemistry when determining the impact of ocean acidification on shallow nearshore marine and estuarine ecosystems.

Competing Interests

JWR is a director of Aquation Pty Ltd.

Acknowledgements

This paper is contribution number 209 from the Sydney Institute of Marine Science.

References

Caldwell, P. C., Merrfield, M. A., and Thompson, P.R. Sea level measured by tide gauges from global oceans — the Joint Archive for Sea Level holdings (NCEI Accession 0019568), Version 5.5, *NOAA National Centers for Environmental Information*, Dataset, doi:10.7289/V5V40S7W, 2015

Dickson, A. G., and Millero, F. J. A comparison of the equilibrium constants for the dissociation of carbonic acid in seawater media. Deep-Sea Res, 34:1733-1743, doi:10.1016/0198-0149(87)90021-5. 1987

Dickson, A. G., Sabine, C. L., and Christian, J. R. Guide to best practices for ocean CO2 measurements. PICES Special Publication, pp 191, 2007.

Hendriks, I. E., Duarte, C. M., Olsen, Y. S., Steckbauer, A., Ramajo, L., Moore, T. S., Trotter, J. A. and McCulloch, M. Biological mechanisms supporting adaptation to ocean acidification in coastal ecosystems. Estuar Coast Shelf S,152:A1–A8, https://doi-org.ezproxy1.library.usyd.edu.au/10.1016/j.ecss.2014.07.019, 2015

Huber, C., Klimant, I., Krause, C., and Wolfbeis, O. S. Dual Lifetime Referencing as Applied to an Optical Chloride Sensor, Anal. Chem., 73:2097-2103, 2001

Johnson, K. S., Jannasch, H. W., Coletti, L. J., Elrod. V. A., Martz, T. R., Takeshita, Y., Carlson, R. J., and Connery, J. G. Deep-Sea DuraFET: A Pressure Tolerant pH Sensor Designed for Global Sensor Networks. Anal Chem, 88:3249-3256. doi: 10.1021/acs.analchem.5b04653, 2016.

Lenton, A., Tilbrook, B., Matear, R. J., Sasse, T. P., and Nojiri, Y. Historical reconstruction of ocean acidification in the Australian region Biogeosciences, 13:1753–1765, doi:10.5194/bg-13-1753-2016, 2016

Liu, X.; Patsavas, M.C.; Byrne, R.H. Purification and characterization of meta-cresol purple for spectrophotometric seawater pH measurements. Environ. Sci. Technol., 45:4862–4868, doi:10.1021/es200665d, 2011.

Martz, T. R., Connery, J. G., and Johnson, K. S.: Testing the Honeywell Durafet (R) for seawater pH applications. Limnol Oceanogr-Meth., 8:172-184, doi:10.4319/lom.2010.8.172, 2010.

Millero, F.J. Thermodynamics of the carbon dioxide system in the oceans. Geochim Cosmochim Ac 59:661-677, doi:10.1016/0016-7037(94)00354-O, 1995

Santos, I. R., Eyre, B. D., and Huettel, M. The driving forces of porewater and groundwater flow in permeable coastal sediments: A review. Estuar Coast Shelf S 98, 1-15, doi.org/10.1016/j.ecss.2011.10.024, 2012.

Schulz, K. G. and Riebesell, U. Diurnal changes in seawater carbonate chemistry speciation at increasing atmospheric carbon dioxide. Mar Biol, 160:1889–1899, DOI 10.1007/s00227-012-1965-y, 2013

Takeshita, Y, Frieder, C. A, Martz, T. R., Ballard, J. R., Feely, R. A., Kram, S., Nam, S., Navarro, M. O., Price, N. N., and Smith, J. E. Including high-frequency variability in coastal ocean acidification projections. Biogeosciences. 12:5853-5870,. doi:10.5194/bg-12-5853-2015, 2015

Biogeosciences Discuss., https://doi.org/10.5194/bg-2017-222
Manuscript under review for journal Biogeosciences
Discussion started: 7 June 2017

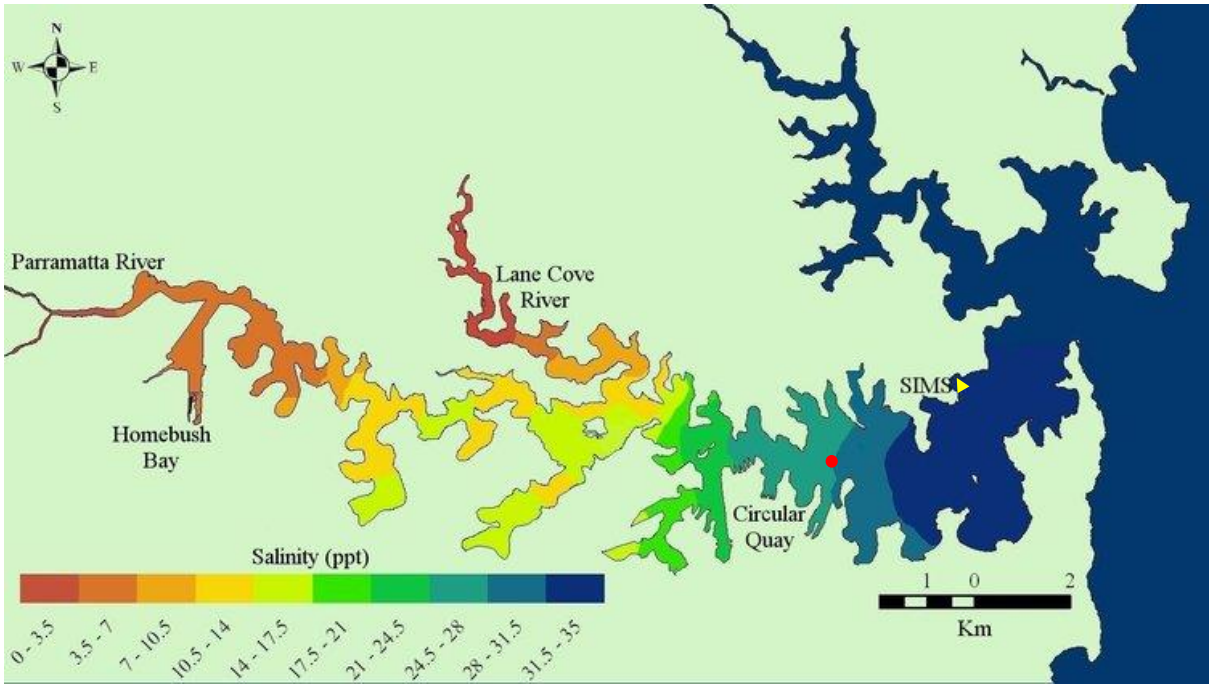

Figure 1. Port Jackson (Sydney Harbour) with sampling site (SIMS, yellow triangle) and Fort Denison tide reference station (red circle). Map courtesy of http://www.sydneyharbourobservatory.org/.

Biogeosciences Discuss., https://doi.org/10.5194/bg-2017-222
Manuscript under review for journal Biogeosciences
Discussion started: 7 June 2017

Figure 2. Submersible logging pH monitor. The fluorescence spot is located on the upper faceplate between and forward of the two submersible connectors, beneath a clear plastic ring.

Biogeosciences Discuss., https://doi.org/10.5194/bg-2017-222
Manuscript under review for journal Biogeosciences
Discussion started: 7 June 2017

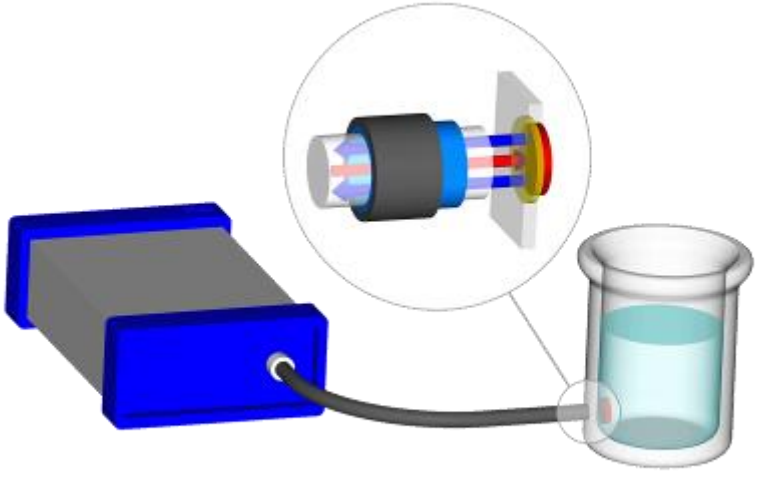

Figure 3. Schematic of pH monitoring system with EOM-pH-mini (left), and fibre optic conveying light to fluorescent spot attached to inside of vessel (right). The insert shows light conveyed through the transparent vessel wall to the spot, and fluorescent light emitted from the spot back along the fibre.

Biogeosciences Discuss., https://doi.org/10.5194/bg-2017-222
Manuscript under review for journal Biogeosciences
Discussion started: 7 June 2017

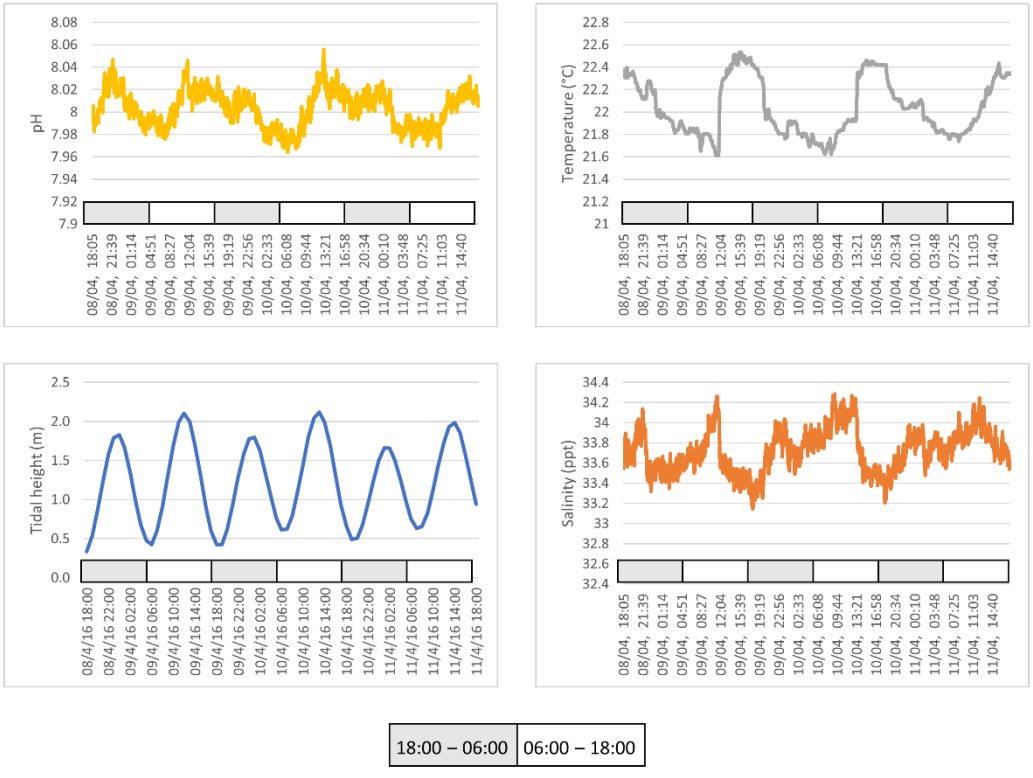

Figure 4. pH, temperature, tidal height and salinity of seawater pumped from ~1 m below low water at Chowder Bay, Sydney over a three-day period. Grey and white boxes indicate the time of day, with grey representing 1800 to 0600 and white representing 0600 to 1800.

Biogeosciences Discuss., https://doi.org/10.5194/bg-2017-222
Manuscript under review for journal Biogeosciences
Discussion started: 7 June 2017

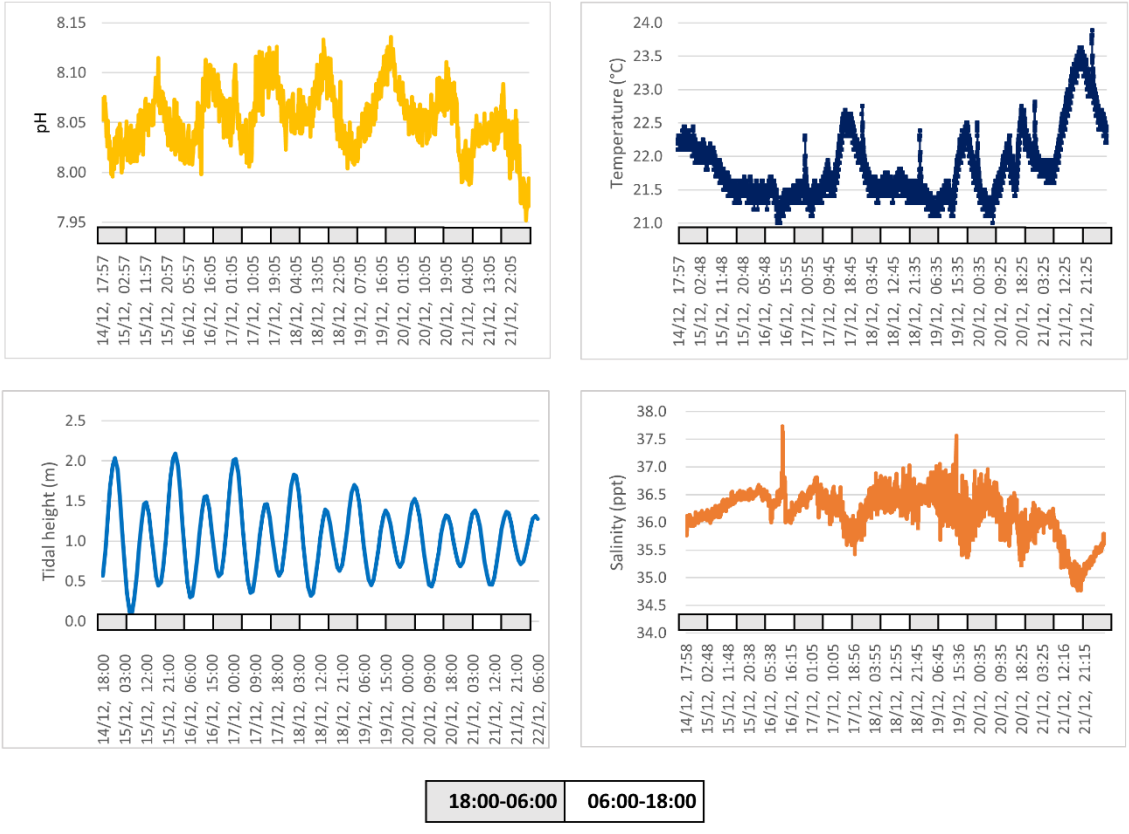

Figure 5. pH, temperature, tidal height and salinity of seawater measured *in situ* at ~1 m below low water at Chowder Bay, Sydney over a multi-day period. Grey and white boxes indicate the time of day, with grey representing 1800 to 0600 and white representing 0600 to 1800.

Biogeosciences Discuss., https://doi.org/10.5194/bg-2017-222
Manuscript under review for journal Biogeosciences
Discussion started: 7 June 2017

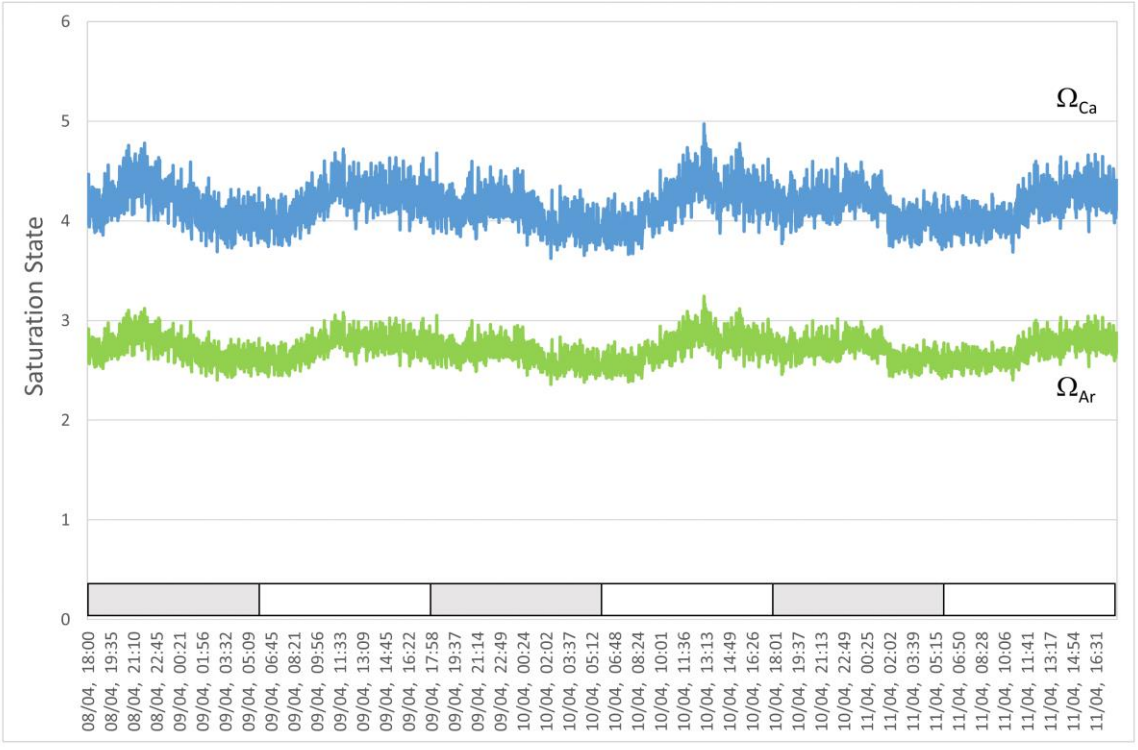

Figure 6. Aragonite and calcite saturation values calculated from data presented in Fig. 2. Values below unity represent dissolution. Grey and white boxes indicate the time of day, with grey representing 1800 to 0600 and white representing 0600 to 1800.

Biogeosciences Discuss., https://doi.org/10.5194/bg-2017-222
Manuscript under review for journal Biogeosciences
Discussion started: 7 June 2017

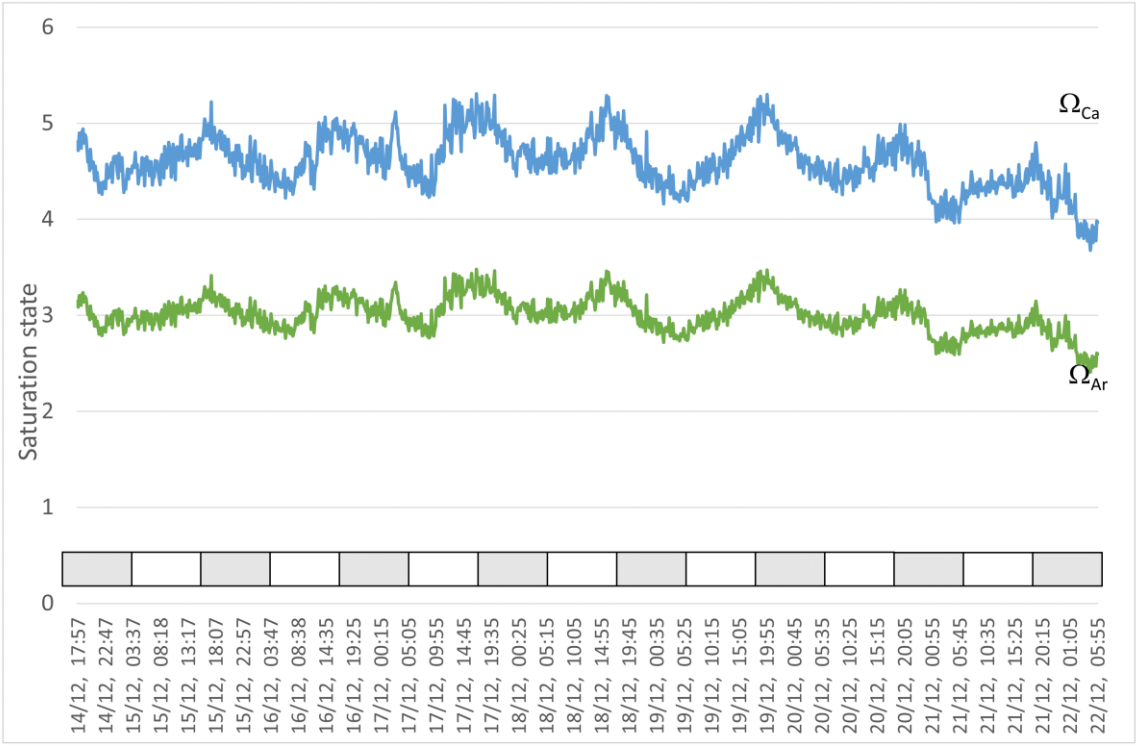

Figure 7. Aragonite and calcite saturation values calculated from data presented in Fig. 4. Values below unity represent dissolution. Grey and white boxes indicate the time of day, with grey representing 1800 to 0600 and white representing 0600 to 1800.